HHS Public Access

Author manuscript

Sci Transl Med. Author manuscript; available in PMC 2020 October 29.

Published in final edited form as:

Sci Transl Med. 2018 December 12; 10(471): . doi:10.1126/scitranslmed.aau0417.

MEK inhibition enhances oncolytic virus immunotherapy through increased tumor cell killing and T cell activation

Praveen K. Bommareddy[1,2], **Salvatore Aspromonate**[2], **Andrew Zloza**[2], **Samuel D. Rabkin**[3], **Howard L. Kaufman**[4,5,*]

[1]School of Graduate Studies, The State University of New Jersey, New Brunswick, NJ 08901 USA,

[2]Rutgers Cancer Institute of New Jersey, Rutgers, The State University of New Jersey, New Brunswick, NJ 08901 USA,

[3]Department of Neurosurgery, Massachusetts General Hospital, Boston, MA 02114 USA

[4]Division of Surgical Oncology, Massachusetts General Hospital, Boston, MA 02114 USA

[5]Replimune, Inc., Woburn, MA 01801 USA

Abstract

Melanoma is an aggressive cutaneous malignancy but advances over the past decade have resulted in multiple new therapeutic options, including molecularly targeted therapy, simmunotherapy and oncolytic virus therapy. Talimogene laherparepvec (T-VEC) is a herpes simplex-1 oncolytic virus and trametinib is a MEK inhibitor approved for treatment of melanoma. Therapeutic responses with T-VEC are often limited and BRAF/MEK inhibition is complicated by drug resistance. We observed that combination T-VEC and trametinib resulted in enhanced melanoma cell death *in vitro*. Further, combination treatment resulted in delayed tumor growth and improved survival in mouse models. Tumor regression was dependent on activated CD8+ T cells and Batf3+ dendritic cells. We also observed antigen spreading and induction of an inflammatory gene signature, including increased expression of PD-L1. Triple therapy with combination T-VEC, MEK inhibition, and anti-PD-1 antibody further augmented responses. These data support clinical development of combination oncolytic viruses, MEK inhibitors and checkpoint blockade in patients with melanoma.

Overline: Cancer

*Address all correspondence to: Howard L. Kaufman, Division of Surgical Oncology, Massachusetts General Hospital, 55 Fruit Street, Boston, MA 02114, 857-250-9928, HLKaufman@mgh.harvard.edu.

Author Contributions

Conceptualization, P.K.B and H.L.K.; Methodology, P.K.B., A.Z., S.D.R. and H.L.K.; Investigation, P.K.B; Technical assistance S.A. Formal Analysis, P.K.B, S.A., A.Z., S.D.R. and H.L.K.; Writing – Original Draft, P.K.B. and H.L.K.; Writing – Review & Editing, P.K.B., A.Z., S.D.R. and H.L.K.; Visualization, P.K.B. and H.L.K.; Funding Acquisition, H.L.K.; Resources, A.Z., S.D.R. and H.L.K.; Supervision, A.Z. and H.L.K.

Competing Interests

H.L.K is an employee of Replimune, Inc. H.L.K and P.K.B are inventors on the patent application submitted by Rutgers University that covers the use of T-VEC, MEK inhibitors and PD-1 blockade (U.S. Provisional Patent Application No. 62/666,390, filed 03 May 2018). S.D.R. is an inventor on patents relating to oncolytic HSV owned by Georgetown University and Massachusetts General Hospital that have been licensed to Amgen, for which he receives royalties, and is also a paid consultant for Replimune, Inc.

Summary: Combining oncolytic virus and a MEK inhibitor augments immune-mediated therapeutic responses in melanoma and enhances sensitivity to PD-1 blockade in mice.

Introduction

Melanoma is a metastatic tumor arising from melanocytes located in the stratum basale of the epidermis, mucosal membranes, and middle layer of the uvea. Metastatic melanoma has historically been associated with dismal prognoses, however systemic therapies have transformed patient outcomes over the past decade, largely due to advances in molecular therapy targeting the RAS-RAF-MEK-ERK mitogen activated protein kinase (MAPK) pathway in patients with tumors that harbor BRAF V600E/K mutations, and by immunotherapy, most notably with immune checkpoint blockade targeting cytotoxic T lymphocyte antigen 4 (CTLA4) and programmed cell death 1 (PD-1) (1). Combination approaches within drug classes have shown improved therapeutic benefit but treatment is associated with drug resistance in the case of MAPK inhibitors, and increased toxicity with checkpoint blockade (2, 3). New combination strategies with agents that enhance therapeutic responses while limiting toxicity have become a high priority for drug development in melanoma.

Oncolytic viruses are a class of cancer drugs that utilize native or genetically modified viruses that selectively replicate in tumor cells(4). Oncolytic viruses mediate therapeutic activity through multiple mechanisms, including direct immunogenic tumor cell killing, release of soluble tumor antigens, danger signals and type 1 interferons, and induction of host anti-tumor immunity (4). Talimogene laherparepvec (T-VEC) is an oncolytic herpes simplex virus, type 1 (HSV-1) encoding granulocyte-macrophage colony-stimulating factor (GM-CSF) and is approved for local treatment of advanced melanoma that has recurred after initial surgery (5). T-VEC has recently been combined with immune checkpoint inhibitors and was associated with improved response rates without an increase in immune-related adverse events (6, 7). The ability of oncolytic viruses to correct various aspects of tumor-mediated immune suppression and the favorable therapeutic window suggest that oncolytic viruses may be ideal candidates for combination approaches with other systemic agents as well. (8).

Approximately 40–50% of cutaneous melanomas harbor mutations in BRAF, which serve as oncogenic drivers of the MAPK pathway promoting tumor progression. Small molecule inhibitors of BRAF and MEK in treatment-naïve melanoma patients whose tumors harbor V600E or V600K BRAF mutations contribute to significant improvements in relapse-free and overall survival (9). Pre-clinical studies have further suggested improved therapeutic activity of combination MAPK inhibition and immune checkpoint blockade (10). Although these findings await further clinical validation, the potential for combining MAPK inhibition with immunotherapy is particularly appealing since MAPK inhibitors act directly on mutated tumor cells resulting in release of soluble tumor-associated antigens while immunotherapy acts on immune cells to promote innate and adaptive immune responses and/or prevent suppression of host anti-tumor immunity (11). Pre-clinical studies have suggested improvements in therapeutic anti-tumor activity between oncolytic viruses and

MEK inhibition in a murine breast cancer model (12). The combination of MEK inhibition and oncolytic viruses has not been tested in melanoma and has not yet entered clinical trials. Thus, we hypothesized that MEK inhibition would improve oncolytic virus responses in melanoma and sought to test this with currently approved agents in melanoma.

Results

Combination MEK Inhibition and Oncolytic Virus Treatment Augments Oncolytic Activity and Viral Replication in Human and Mouse Melanoma cell lines

We sought to investigate whether combining T-VEC and MAPK inhibition can augment tumor cell killing in melanoma. T-VEC was able to replicate in and kill melanoma cell lines harboring BRAF V600E mutations and wild-type N-Ras (SK-MEL-28 and SK-MEL-5; Suppl. Fig. 1A–B) and those cells with wild-type BRAF, but an NRAS Q61R mutation (SK-MEL-2; Suppl. Fig. 1C). Infected cells exhibited dose-dependent cytotoxicity following viral infection at doses starting at 0.003 multiplicity of infection (MOI) (Suppl. Fig. 1A–C). In addition, the BRAF-mutated murine D4M3A cell line (13) was susceptible to T-VEC at high doses (MOI ≥ 1; Suppl. Fig. 1D). Cytotoxicity was increased in all cell lines when they were pre-treated with trametinib, a selective MEK inhibitor (MEKi; Fig. 1A–D, left panel). Independent assays with vemurafenib, a selective BRAF inhibitor, enhanced T-VEC-mediated cytotoxicity in BRAF V600E mutated SK-MEL-28 and SK-MEL 5 cell lines, but not in BRAF wild-type SK-MEL-2 line (Suppl. Fig. 1E–G). Increased viral replication was confirmed by plaque assay (Fig. 1A–D right panels) and Western blot showing increased amounts of HSV-1 glycoprotein D during combination treatment in the SKMEL-28 cell line (Fig. 1E).

In order to confirm viral replication within infected cells we utilized single-cell laser radiance-based quantitative technology (14) that allows detection of viral infection at a single cell level (Suppl. Fig. 2A). As shown in Figure 1F, the infection metric was increased at 18 hours for virally infected cells with the highest value seen in cells treated with T-VEC and MEKi (Fig. 1F, left). A time-course analysis on cells infected with T-VEC at low (0.01) or high (1.0) MOI or uninfected control cells showed the expected rapid increase in infection metric for cells infected with 1 MOI, while cells infected with 0.01 MOI demonstrated a delayed increase in infection metric at 36 hours when more virus had replicated (Fig. 1F, right). Principal component analysis (PCA) based on cell size (F1) and radiance (F2) was able to differentiate each of the treated cell populations (Fig. 1G).

T-VEC and MEK Inhibition Inhibits Tumor Growth in Melanoma Xenograft Model.

Next, we sought to determine if T-VEC and MEK inhibition had therapeutic activity aga *in vivo*. We utilized a murine xenograft model using the human SK-MEL-28 cell line (Fig. 2A). Delayed tumor growth was observed with MEK inhibition alone and T-VEC alone, but combination treatment was associated with a significant decrease in tumor growth and tumor regression compared to mock or monotherapy treatments ($p < 0.001$; Fig. 2B). Previously, MEK inhibition was shown to induce tumor cell apoptosis (15), therefore, we sought to determine how cells were killed in this model. We found combination of T-VEC and MEKi is associated fewer proliferating cells, based on Ki-67 immunostaining, compared to either

treatment alone(Fig. 2C). HSV-1 in tumors was detected by immunostaining for the HSV-1 glycoprotein D, which was seen in the T-VEC alone-treated tumors and significantly increased in tumors of mice treated with T-VEC and MEKi (Fig. 2D). We also observed decreased levels of phosphorylated (p)ERK in tumor cells treated with MEKi, as well as tumors treated with T-VEC alone, which was further decreased in tumors treated with the combination (Fig. 2E). Finally, while T-VEC treatment alone resulted in significant increase in caspase 3 cleavage compared to mock treatment, combination therapy resulted in higher tumor cell apoptosis *in vivo* (Fig. 2F).

To confirm melanoma cell apoptosis, we treated SK-MEL-28 cells *in vitro* and found an increase in Annexin-V staining in cells treated with the combination compared to monotherapy or mock treatment (Suppl. Fig. 3A–B), and this effect was partially blocked by a pan-caspase inhibitor (Z-VAD),(Suppl. Fig. 3C). Further, there was increased cleaved PARP in tumor cells treated with both T-VEC and trametinib (Suppl. Fig 3D). Collectively, these data demonstrate that combination T-VEC and MEK inhibition can delay melanoma xenograft growth *in vivo* and that treatment is associated with decreased tumor cell viability and increased apoptosis.

T-VEC and MEK Inhibition Enhances Therapeutic Effectiveness and Improves Survival in the Immune-competent D4M3A Murine Melanoma model

To determine the effects of combination T-VEC and trametinib (MEKi) in an immune-competent D4M3A BRAFV600E melanoma model, we used a modified T-VEC encoding murine GM-CSF (mT-VEC), as described in the Materials and Methods. D4M3A cells are susceptible to T-VEC infection and killing (Suppl. Fig. 4A) and exhibit upregulation of pERK, characteristic of BRAFV600E mutated cells (Suppl. Fig. 4B). In D4M3A tumor-bearing mice, mT-VEC alone exhibited no significant delays in tumor growth (Fig 3B–C) while MEKi (MEKi) alone showed significant delays in tumor growth (Fig. 3B–C). Combination treatment, however, was associated with significant tumor growth inhibition and improved survival with complete tumor eradication in 4 of 9 (44%) mice (Fig. 3C). Mice with complete tumor regression remained tumor free (Fig. 3C) and were re-challenged with twice the number of D4M3A cells implanted in the opposite flank (left). In this experiment, 70% (5/7) of mice completely rejected re-challenged tumor (Fig. 3D). We further observed a significant increase in tumor infiltrating $CD8^+$ T cells in mice treated with combination therapy (Fig. 3E). $CD8^+$ T cells exhibited increased levels of interferon-γ, Granzyme B and Ki-67 (Fig. 3E), indicative of an activated cytotoxic phenotype (Fig. 3E). The increased number of $CD8^+$ T cells was further confirmed by immunohistochemistry (Fig. 3F–G). Both mT-VEC and MEKi demonstrated an increase in $CD8^+$ T cells following treatment, which were further increased by combination therapy (Fig. 3F–G). There was no significant change in the total number of $CD3^+CD4^+$ T cells (Fig. 3H), but there was a decrease in $CD4^+FoxP3^+$ regulatory T cells (Tregs) in mice treated with mT-VEC alone or in combination with MEKi (Fig. 3H). This resulted in a significant increase in the $CD8^+$/Treg ratio in mice treated with mT-VEC alone and in combination with MEKi (Fig. 3H).

T-VEC and MEKi Combination Therapy is CD8+ T cell-dependent

To determine which immune cells are involved in the anti-tumor activity, we repeated the *in vivo* tumor experiments using depletion antibodies against $CD4^+$ and $CD8^+$ T cells, and liposomal clodronate to deplete macrophages. All cell depletions were confirmed by FACS analysis of splenocytes (Suppl. Fig. 5A–B). Mice bearing D4M3A tumors were treated as described in the survival experiments in Fig. 3 and depletion antibodies were injected as shown in (Fig. 4A) and described in Materials and Methods. Neither macrophage depletion nor $CD4^+$ T cell depletion significantly impacted anti-tumor activity, but $CD8^+$ cell depletion completely abrogated the anti-tumor activity and survival benefit (Fig. 4B–C). FACS analysis confirmed the loss of $CD4^+$ and $CD8^+$ T cells in tumors collected from mice treated with immune cell depleting antibodies (Fig 4D, E). A compensatory increase in $CD4^+$ T cells in the tumor microenvironment of mice depleted of $CD8^+$ cells (Fig. 4D) and increased $CD8^+$ T cells in tumors of mice depleted of $CD4^+$ cells (Fig 4E) was seen.

Combination treatment with T-VEC and MEKi augments melanoma antigen-specific T cell responses

We sought to further characterize the antigen specificity of the $CD8^+$ T cell responses in mice treated with mT-VEC/MEKi combination therapy. Initially, flow cytometry using MHC-I dextramers for two defined melanoma antigens, gp100 and TRP2 and one viral antigen,HSV-1 gB, was used to determine antigen specificity of tumor infiltrating $CD8^+$ T cells during T-VEC treatment alone in a time course study (Suppl. Fig. 6). We saw an initial increase of HSV-1 gB-specific $CD8^+$ T cells at day 19 which plateaued by day 24 (Suppl. Fig. 6). Gp100- and TRP2-specific $CD8^+$ T cells emerged between days 19–24 (Suppl. Fig. 6). mT-VEC treatment induced HSV-1 gB-specific $CD8^+$ T cells (Fig. 5A) and combination mT-VEC and MEKi resulted in a significant increase in the relative frequency of tumor-infiltrating HSV-1 gB-specific $CD8^+$ T cells (Fig. 5A). We also observed an increase in gp100- and TRP2-specific $CD8^+$ T cells during combination treatment (Fig. 5B–C). Although the increase in melanoma-specific $CD8^+$ T cells was especially high within the tumor-infiltrating lymphocyte population, we did not detect HSV-1-specific $CD8^+$ T cells in the spleen of treated animals but did observe a minimal, but significant, increase in both gp100- and TRP2-specific $CD8^+$ T cells in the spleen (Suppl. Fig. 7). These data suggest that T-VEC and MEKi can induce antigen spreading.

Combination treatment with T-VEC and MEKi is Dependent on Batf3+ Dendritic Cells.

To determine the role of CD8+CD103+ DCs in mediating anti-tumor immunity (16, 17)., we implanted D4M3A tumors into $Batf3^{-/-}$ mice. The lack of $CD8^+CD103^+$ DCs in $Batf3^{-/-}$ mice did not alter the ability to establish D4M3A tumors (Suppl. Fig. 8A, B). Tumors from $Batf3^{-/-}$ mice had significantly reduced frequency of $CD45^+MHCII^+CD11c^+CD103^+$ cells, as well as $CD45^+MHCII^+CD11c^+CD8^+$ cells after combination therapy (Suppl. Fig. 8C). To determine the effects of $Batf3^+$ DCs on combination therapy, D4M3A tumors were implanted in C57BL/6J and $Batf3^{-/-}$ mice and treated as described in Fig. 3. Although combination treatment resulted in delayed tumor growth in C57BL/6J mice, as previously seen (Fig. 3C), this effect was significantly diminished in $Batf3^{-/-}$ mice (Fig. 6A–B).

Treated Batf3$^{-/-}$ mice demonstrated a significant decrease in the percent and number of CD8^{+} T cells compared to C57BL/6J (B6) (Fig. 6C). There was also a significant decrease in the percent of CD8^{+} T cells expressing IFN-γ and Granzyme B (Fig. 6D) and proliferating (Ki67^{+}) CD8^{+} T cells (Fig. 6D) and increased Tregs, (Fig. 6E) seen after combination treatment. We also observed a significant decrease in gB-specific CD8^{+} T cells and gp100- and TRP2-specific CD8^{+} T cells in Batf3$^{-/-}$ mice compared to wild-type mice treated with combination therapy (Fig. 6F).

Combination T-VEC and MEK Inhibition Induces an Inflammatory Gene Signature and Increases PD-L1 Expression in the Tumor Microenvironment

Previous studies have identified an inflammatory gene signature in patients responding to PD-1 checkpoint blockade (18). Since T-VEC is associated with type 1 interferon release and CD8^{+} T cell recruitment to the tumor microenvironment, we evaluated the established D4M3A tumors on day 24 from mice treated with mT-VEC, MEKi or both for inflammatory gene expression profile. Treatment with mT-VEC was associated with an increased inflammatory signature compared to both mock- and MEKi-treated tumors, and that this profile was highest in tumors treated with combination mT-VEC and MEKi (Fig. 7A). We also restricted the gene expression profile to 5 genes related to T cell activation (*interferon-γ, CD8α, tumor necrosis factor-α, granzyme B* and *perforin 1*) and found a correlation between T cell activation gene expression and therapeutic effects (Fig. 7B; Suppl. Fig. 9A), as well as categories of genes related to immune cells and anti-viral immunity (Suppl. Fig 9B–C). While MEKi inhibited expression of most anti-viral genes, the combination of mT-VEC and MEKi resulted in increased gene expression compared to mT-VEC alone, except for *interleukin-34* (IL34) and *NKG2D ligand* (UL16 binding protein 1; Ulbp1).

While PD-1 and PD-L1 expression was significantly increased in the inflammatory gene panel in T-VEC and MEK inhibitor-treated animals (Fig. 7C), this was confirmed by flow cytometry analysis of CD45^{+} cells harvested from the tumor microenvironment at day 24 as described in Fig. 3D. An increase in both PD-1 and PD-L1 was observed in tumors treated with mT-VEC alone, but they were highest in tumors treated with the combination (Fig. 7D).

Triple Treatment with T-VEC, MEK Inhibition and PD-1 Blockade Further Enhances Therapeutic Activity.

Although combination therapy using mT-VEC and MEK inhibition reduced tumor burden and enhanced survival of treated mice (Fig. 3B, C), tumors were completely eradicated in only 30–40% of mice. Based on the flow cytometry analysis and gene expression profiling showing an increase in PD-1 and PD-L1 expression in the tumor microenvironment (Fig. 7D), we reasoned the that therapeutic activity might be further expanded by addition of PD-1 blockade to the combination regimen. To test this, we treated D4M3A tumor-bearing mice with mT-VEC, MEKi, or both as previously described in Fig. 3C, and with or without αPD-1 antibody. There was limited impact of αPD-1 when given with mT-VEC alone or MEK inhibition alone (Fig 8B, C), as compared to monotherapy (Fig 3B, C). However, the combination of αPD-1 with both mT-VEC and MEKi resulted in complete durable responses in almost all mice (6/7), compared to 2/7 mice with mT-VEC and MEKi (Fig. 8C). All mice who cleared primary tumors with mT-VEC/MEKi/αPD-1 therapy rejected

subsequent tumor re-challenge (Fig. 8D). Flow cytometry analysis performed on tumors showed a significant decrease in $CD45^+PD\text{-}1^+$ and $CD8^+PD\text{-}1^+$ cells in mice treated with triple therapy compared to mT-VEC and MEKi (Fig. 8E, Suppl. Fig. 10). No significant changes were observed in Tregs or the $CD8^+$/Treg ratio (Fig. 8F). Triple combination elicited an increase in the percentage of total $CD8^+$ T cells (Fig 8G, left panel), as well as granzyme B and Ki67 expression (Fig 8G). There was no overt toxicity observed in the mice as evidenced by changes in body weight, feeding habits, stool frequency or coat appearance, including the absence of vitiligo.

Finally, to test the efficacy of triple combination in a different model we tested the triple combination in BALB/c mice bearing established CT26 murine colon cancer tumors. In the CT26 model, both mT-VEC/MEKi and mT-VEC/αPD-1 antibody dual combinations elicited significant anti-tumor activity, with regression observed in 5/10 mice (Fig 8H, Suppl. Fig. 11). In addition, the triple combination, using mT-VEC/MEKi/αPD-1, caused regression of all tumors, producing complete responses not observed with double therapy treatment (Fig 8H, Suppl. Fig. 11). There were no signs of toxicity or weight loss in any of these animals.

Discussion

In this report, we demonstrate that the combination of T-VEC and MEK inhibition increases melanoma tumor cell killing through increased viral replication and apoptosis in vitro and enhances melanoma-specific adaptive immune responses in vivo. Previous reports have described interactions between MAPK pathway inhibition and othert oncolytic viruses (12, 19). MEK inhibition was found to increase oncolytic adenovirus replication and tumor cell killing, possibly through upregulation of coxsackievirus and adenovirus receptor (20). In glioma cells, MEKi PD98059 inhibited autophagy and increased cell killing without increasing oncolytic adenovirus replication (21). Oncolytic reovirus increased tumor cell killing due to increased endoplasmic reticulum stress-induced apoptosis and not increased virus replication (19). The effects of MEK inhibition are more complex with oncolytic HSV and depend on the particular virus strain. An internal repeat-deleted oncolytic HSV-1 inhibited p-MAPK activation *in vitro* and synergized with PD98059 in killing triple negative breast cancer cell lines (12). In contrast, the tumor cell cytotoxicity of ICP34.5-deleted oncolytic HSV-1 (R3616) in vitro correlated with constitutive MEK activation, due to suppression of protein kinase R so that MEK inhibition reduced virus replication by about 15-fold (22). The R3616 virus was also found to be more effective *in vivo* against tumors with high MEK activity (23). Compared to R3616, T-VEC has an additional ICP47 deletion, resulting in early Us11 expression and PKR suppression, which likely explains the favorable interaction of T-VEC with MEKi. Thus, different oncolytic viruses interact with MEK inhibition in different ways.

In our model we utilized trametinib, which is a more selective MEK 1/2 inhibitor and has been previously shown to have fewer side effects compared to other MEK inhibitors (24). Thus, in the context of combination therapy, trametinib might provide particulalry improved therapeutic window. Another factor known to influence the replicative ability of viruses is the status of the anti-viral machinery, which is composed of intra-cellular factors that detect viral nucleic acids and molecular elements that promote viral clearance, such as type 1

interferon, and viral DNA sensors such as cGAS-STING. The expression of the anti-viral machinery is typically defective in tumor cells, which allows preferential replication for many oncolytic viruses (25). In our model, we also confirmed that MEK inhibition was associated with decreased anti-viral response expression *in vivo*, including STING (Tmem173) and interferon response factors (IRFs) 3 and 7. MEK inhibition inhibits expression of these factors, thus establishing favorable intra-cellular conditions for viral replication.

While MEK inhibition in tumor cells may promote apoptosis and drive immunogenic cell death, MEK inhibition may also block T cell activation (26). Thus, it may be surprising that we observed strong anti-viral and anti-tumor $CD8^+$ T cell responses in our model (Figs 3 and 5). One explanation may have related to a recent finding that MEK inhibition selectively blocks activation of naïve T cells but not antigen-experienced effector T cells (10). Others have shown that MEK inhibition selectively suppresses alloreactive T cells in a model of graft-versus-host disease, demonstrating that trametinib blocks GVHD-inducing CD8+ T cells but spares graft-versus-tumor-specific CD8+ T cells *in vivo* (27). Thus, established tumors may contain antigen-experienced T cells and, in this setting, MEK inhibition would be expected to promote T cell activation, consistent with the Nanostring data from tumor bearing mice treated with trametinib and mT-VEC. The increased expression of STING and TLRs may also promote recruitment of anti-tumor $CD8^+$ T cells as induction of these innate immune sensors has been associated with restoration of effective anti-tumor immunity (28).

Another important observation in our study was that BRAF inhibition only enhanced T-VEC oncolysis in BRAF-mutant tumor cells. In contrast, MEK inhibition improved T-VEC replication and oncolytic activity in both BRAF-mutant and BRAF wild-type cell lines. This suggests that MEK inhibition may be better than BRAF inhibitors in combination with HSV-based OV therapy and might be active regardless of BRAF mutation status. This will, however, require further clinical validation.

In our studies, therapeutic effectiveness was seen in both human xenograft and immune-competent melanoma models. We found that combination T-VEC and MEK inhibition is also associated with increased accumulation of activated CD8+ T cells, characterized by production of IFN-γ and Granzyme B, within the tumor microenvironment as well as an increase in CD8+/Treg ratio. We also confirmed the importance of $CD8^+$ T cells through selective immune cell depletion studies. This is consistent with prior reports in melanoma patients treated with single-agent T-VEC in which injected tumors have been found to have higher numbers of MART-1-specific effector CD8+ T cells and decreased numbers of CD4+ Foxp3+ Tregs (29). Since HSV-1 can promote IFN production, we also found an increase in PD-1 and PD-L1 expression within the tumor microenvironment (30)and this is likely related to the counter-regulatory induction of immune checkpoints in the setting of excessive IFN-γ (31). This comports with recent clinical data showing increased PD-L1 expression in tumors from melanoma patients treated with T-VEC and pembrolizumab (6) and provides a biologic rationale for the addition of PD-1 blockade to T-VEC and MEKi treatment, where we showed over 80% complete tumor eradication and increased survival without overt signs of toxicity. This triple drug regimen is particularly appealing since all three agents are currently FDA-approved for the treatment of melanoma, and it is consistent with recent

reports suggesting MAPK pathway inhibition and PD-1/PD-L1 blockade are associated with improved therapeutic responses in pre-clinical models (10, 32).

The Batf3$^+$ (CD8$^+$CD103$^+$) DC population was initially identified as critical for priming anti-viral CD8$^+$ T cells responses (16). These DCs are also critical for anti-tumor immunity and recruitment of lymphocytes through chemokines, such as CXCL9 (33). We demonstrated that Batf3$^+$ DCs are also critical for the recruitment of CD8$^+$ T cells in our melanoma model following treatment with T-VEC and trametinib, and observed an increase in CXCL9 expression. These data support a role for Batf3$^+$ DCs and local CXCL9 expression to generate and recruit effector CD8$^+$ T cells into the tumor microenvironment. We found evidence for both viral (HSV gB-specific) and melanoma (gp100- and TRP2-specific) CD8$^+$ T cell responses, consistent with initial viral responses followed by cross presentation of tumor-associated antigens (34). Antigen spreading has previously been reported as a predictive biomarker of therapeutic responses for other forms of immunotherapy, including tumor vaccines and immune checkpoint inhibitors (35, 36). We further observed that combination therapy promoted an IFN-γ-regulated gene signature profile that has been associated with therapeutic responses to PD-1 blockade in patients with melanoma (18). Based on the increased expression of PD-1 and PD-L1, we added anti-PD-1 therapy to the mT-VEC+MEKi combination, which resulted in a survival benefit. We also observed a similar therapeutic effect for triple combination in the genetically distinct BALB/c murine CT26 model suggesting that this approach may be broadly applicable for solid tumors beyond melanoma. Finally, our data may also have implications for other microbial pathogens being evaluated as cancer therapeutics. In a patient-derived orthotopic xenograft model, treatment with *Salmonella typhimurium* combined with vemurafenib or trametinib resulted in improved therapeutic responses in a BRAF V600E mutated melanoma (37).

Our study does have certain limitations, such as the use of murine models for oncolytic virus studies, which may be influenced by decreased viral tropism in murine tumor cells compared to human tumor cells. In addition, xenograft models are not adequate for representing an intact host immune system and implanted tumors may not adequately reflect the biology of spontaneously arising cancers. We did observe infection of the D4M3A cell line, which allowed therapeutic studies to be conducted and these were supplemented with human xenograft tumor experiments, which are susceptible to T-VEC infection and treatment with MEKi.

In summary, we evaluated the combination of MAPK inhibition and T-VEC in murine and human melanoma cell lines and found an unexpected synergistic effect between T-VEC and MEK inhibition regardless of BRAF mutation status. We also confirmed that therapeutic responses could be further improved by addition of anti-PD-1 therapy. In our studies, we did not observe overt signs of toxicity in mice supporting an improved therapeutic window although clinical confirmation is needed. Collectively, these data provide pre-clinical rationale for triple combination treatment of T-VEC, MEK inhibition and PD-1 blockade in patients with melanoma.

Material and Methods

Study design

In this hypothesis-driven study, we tested the therapeutic potential of two clinically approved agents in melanoma, an oncolytic virus, talimogene laherparepvec, and the selective MEK inhibitor, trametinib. Combination therapy was evaluated in human and murine melanoma cell lines in vitro, in human-derived xenograft tumor models in vivo, and in a transplantable murine model using the D4M3A cell line that is sensitive to HSV-1 infection. The effect of the two-drug regimen on viral replication was assessed by plaque assay. In addition, immune studies were performed to determine the impact of the combination on various immune cell populations, antigen spreading and induction of gene signature profiles. The initial experiments found that the combination treatment induced expression of PD-1 and PD-L1, and further in vivo studies were conducted to assess triple combination treatment with oncolytic virus, MEK inhibitor and PD-1 blockade. In all experiments, animals were assigned to various experimental groups at random, but investigators were not blinded. For survival studies, sample sizes of 7 to 10 mice per group were used. Mice were euthanized when tumors reached 400 mm^2. All outliers were included in the data analysis.

Cell Lines

Human melanoma cells SK-MEL-28, SK-MEL-2, and SK-MEL-5 (ATCC) and mouse cell line CT26 (ATCC) were cultured in monolayers using RPMI supplemented with 10% heat inactivated bovine serum (Thermo Fisher Scientific), 10mM L-glutamine (Corning), and 0.5% penicillin G-streptomycin sulfate (Corning). Cells were detached using 0.25% trypsin EDTA (Corning) for passaging. The murine melanoma cell line D4M3A was generated from *Tyr::CreER;Braf*^{CA}*;Pten*$^{lox/lox}$ mice (13) and kindly provided by Dr. David Mullins (Dartmouth University, Hanover, NH). D4M3A cells were cultured as previously described (13). All cells were low-passage and confirmed to be mycoplasma-free (LookOut mycoplasma kit; Sigma).

Viruses

T-VEC is a modified JS1 strain of HSV-1 encoding human GM-CSF and has been previously reported (38). T-VEC is commercially available and was purchased from the Rutgers Cancer Institute Pharmacy. For immune competent murine studies, a modified virus (mT-VEC) in which the human GM-CSF gene was replaced by murine GM-CSF, was used and generously provided by Dr. Pedro Beltran (Amgen Inc). All human cell lines and xenograft experiments were performed using T-VEC and all murine cell line and syngeneic experiments were performed using mT-VEC.

Drugs, chemicals and antibodies

Drugs and antibodies and their respective suppliers are listed in table S1. Chemical agents are listed in table S2.

Cytotoxicity and viral plaque assays, Western blotting, Lumacyte analysis, immune histochemistry and flow cytometry

All commercial kits used in these experiments are listed in table S3 and described in more detail in the supplemental methods.

Gene expression studies

Gene expression analysis was performed using the NanoString PanCancer Immune panel as described in supplemental methods.

Murine tumor treatment

The murine treatment and survival studies, as well as the immune cell depletion experiments, are described in detail in the supplemental methods. In tumor treatment studies, tumor growth was measured in two dimensions recording the greatest length and width using digital calipers. Tumor area was calculated by multiplying length and width. Tumor sizes were plotted as average size for each group. For survival experiments mice were monitored for tumor-growth and euthanized when tumors reached 400 mm^2. Kaplan-Meier curves were used to document survival. Mice were weighed twice a week and no weight loss was observed during the treatment. Each experiment was performed at least two times and all animal experiments were approved by Rutgers Institutional Animal Care and Usage Committee.

Statistical Analyses

All statistical analyses were performed using Graphpad Prism software version 7.0a. Survival data were analyzed by Kaplan-Meier survival curves, and comparisons were performed by Log Rank test. Cell viability data, flow cytometric data and immunohistochemistry counts were compared using an unpaired student's t test (two-tailed) or one-way ANOVA when multiple comparisons were done. P values of less than 0.05 were considered significant.

Supplementary Material

Refer to Web version on PubMed Central for supplementary material.

Acknowledgments

The authors wish to thank Drs. Colin Hebert and Sean Hart at Lumacyte and Drs. Pedro Beltran, Jennifer Gansert, and Cooke Keegan at Amgen, Inc. for reagents and research funding. We thank Dr. David Mullins at Dartmouth University for providing D4M3A cell line. We thank Dr. Dipongkor Saha (Rabkin lab) for helpful discussion and useful comments with experimental methods and writing the manuscript. We also thank Dr. Cole Peters (Rabkin lab) for helpful discussions. We thank Dr. Sachin Jhawar, Dr. Shengguo Li, Russell Pepe, Jenna Newman and members of Zloza lab for experimental help and useful discussions. We thank Nano String Technologies for help with gene expression analysis. We also thank Dr. Rob Coffin for useful comments and suggestions.

Funding

H.L.K received partial funding to support this research through a grant from Amgen. S.D.R was supported by NIH grant (R01CA160762) to SDR.

References and Notes

1. Luke JJ, Flaherty KT, Ribas A, Long GV. 2017 Targeted agents and immunotherapies: optimizing outcomes in melanoma. Nat Rev Clin Oncol 14: 463–82 [PubMed: 28374786]
2. Larkin J, Chiarion-Sileni V, Gonzalez R, Grob JJ, Cowey CL, Lao CD, Schadendorf D, Dummer R, Smylie M, Rutkowski P, Ferrucci PF, Hill A, Wagstaff J, Carlino MS, Haanen JB, Maio M, Marquez-Rodas I, McArthur GA, Ascierto PA, Long GV, Callahan MK, Postow MA, Grossmann K, Sznol M, Dreno B, Bastholt L, Yang A, Rollin LM, Horak C, Hodi FS, Wolchok JD. 2015 Combined Nivolumab and Ipilimumab or Monotherapy in Untreated Melanoma. N Engl J Med 373: 23–34 [PubMed: 26027431]
3. Wolchok JD, Chiarion-Sileni V, Gonzalez R, Rutkowski P, Grob JJ, Cowey CL, Lao CD, Wagstaff J, Schadendorf D, Ferrucci PF, Smylie M, Dummer R, Hill A, Hogg D, Haanen J, Carlino MS, Bechter O, Maio M, Marquez-Rodas I, Guidoboni M, McArthur G, Lebbe C, Ascierto PA, Long GV, Cebon J, Sosman J, Postow MA, Callahan MK, Walker D, Rollin L, Bhore R, Hodi FS, Larkin J. 2017 Overall Survival with Combined Nivolumab and Ipilimumab in Advanced Melanoma. N Engl J Med 377: 1345–56 [PubMed: 28889792]
4. Kaufman HL, Kohlhapp FJ, Zloza A. 2015 Oncolytic viruses: a new class of immunotherapy drugs. Nat Rev Drug Discov 14: 642–62 [PubMed: 26323545]
5. Andtbacka RH, Kaufman HL, Collichio F, Amatruda T, Senzer N, Chesney J, Delman KA, Spitler LE, Puzanov I, Agarwala SS, Milhem M, Cranmer L, Curti B, Lewis K, Ross M, Guthrie T, Linette GP, Daniels GA, Harrington K, Middleton MR, Miller WH Jr., Zager JS, Ye Y, Yao B, Li A, Doleman S, VanderWalde A, Gansert J, Coffin RS. 2015 Talimogene Laherparepvec Improves Durable Response Rate in Patients With Advanced Melanoma. J Clin Oncol 33: 2780–8 [PubMed: 26014293]
6. Ribas A, Dummer R, Puzanov I, VanderWalde A, Andtbacka RHI, Michielin O, Olszanski AJ, Malvehy J, Cebon J, Fernandez E, Kirkwood JM, Gajewski TF, Chen L, Gorski KS, Anderson AA, Diede SJ, Lassman ME, Gansert J, Hodi FS, Long GV. 2017 Oncolytic Virotherapy Promotes Intratumoral T Cell Infiltration and Improves Anti-PD-1 Immunotherapy. Cell 170: 1109–19 e10 [PubMed: 28886381]
7. Chesney J, Puzanov I, Collichio F, Singh P, Milhem MM, Glaspy J, Hamid O, Ross M, Friedlander P, Garbe C, Logan TF, Hauschild A, Lebbe C, Chen L, Kim JJ, Gansert J, Andtbacka RHI, Kaufman HL. 2017 Randomized, Open-Label Phase II Study Evaluating the Efficacy and Safety of Talimogene Laherparepvec in Combination With Ipilimumab Versus Ipilimumab Alone in Patients With Advanced, Unresectable Melanoma. J Clin Oncol: JCO2017737379
8. Bommareddy PK, Shettigar M, Kaufman HL. 2018 Integrating oncolytic viruses in combination cancer immunotherapy. Nat Rev Immunol
9. Long GV, Stroyakovskiy D, Gogas H, Levchenko E, de Braud F, Larkin J, Garbe C, Jouary T, Hauschild A, Grob JJ, Chiarion Sileni V, Lebbe C, Mandala M, Millward M, Arance A, Bondarenko I, Haanen JB, Hansson J, Utikal J, Ferraresi V, Kovalenko N, Mohr P, Probachai V, Schadendorf D, Nathan P, Robert C, Ribas A, DeMarini DJ, Irani JG, Casey M, Ouellet D, Martin AM, Le N, Patel K, Flaherty K. 2014 Combined BRAF and MEK inhibition versus BRAF inhibition alone in melanoma. N Engl J Med 371: 1877–88 [PubMed: 25265492]
10. Ebert PJR, Cheung J, Yang Y, McNamara E, Hong R, Moskalenko M, Gould SE, Maecker H, Irving BA, Kim JM, Belvin M, Mellman I. 2016 MAP Kinase Inhibition Promotes T Cell and Anti-tumor Activity in Combination with PD-L1 Checkpoint Blockade. Immunity 44: 609–21 [PubMed: 26944201]
11. Hu-Lieskovan S, Robert L, Homet Moreno B, Ribas A. 2014 Combining targeted therapy with immunotherapy in BRAF-mutant melanoma: promise and challenges. J Clin Oncol 32: 2248–54 [PubMed: 24958825]
12. Gholami S, Chen CH, Gao S, Lou E, Fujisawa S, Carson J, Nnoli JE, Chou TC, Bromberg J, Fong Y. 2014 Role of MAPK in oncolytic herpes viral therapy in triple-negative breast cancer. Cancer Gene Ther 21: 283–9 [PubMed: 24924199]
13. Jenkins MH, Steinberg SM, Alexander MP, Fisher JL, Ernstoff MS, Turk MJ, Mullins DW, Brinckerhoff CE. 2014 Multiple murine BRaf(V600E) melanoma cell lines with sensitivity to PLX4032. Pigment Cell Melanoma Res 27: 495–501 [PubMed: 24460976]

14. Hebert CG, DiNardo N, Evans ZL, Hart SJ, Hachmann AB. 2018 Rapid quantification of vesicular stomatitis virus in Vero cells using Laser Force Cytology. Vaccine
15. Liu L, Mayes PA, Eastman S, Shi H, Yadavilli S, Zhang T, Yang J, Seestaller-Wehr L, Zhang SY, Hopson C, Tsvetkov L, Jing J, Zhang S, Smothers J, Hoos A. 2015 The BRAF and MEK Inhibitors Dabrafenib and Trametinib: Effects on Immune Function and in Combination with Immunomodulatory Antibodies Targeting PD-1, PD-L1, and CTLA-4. Clin Cancer Res 21: 1639–51 [PubMed: 25589619]
16. Hildner K, Edelson BT, Purtha WE, Diamond M, Matsushita H, Kohyama M, Calderon B, Schraml BU, Unanue ER, Diamond MS, Schreiber RD, Murphy TL, Murphy KM. 2008 Batf3 deficiency reveals a critical role for CD8alpha+ dendritic cells in cytotoxic T cell immunity. Science 322: 1097–100 [PubMed: 19008445]
17. Spranger S, Dai D, Horton B, Gajewski TF. 2017 Tumor-Residing Batf3 Dendritic Cells Are Required for Effector T Cell Trafficking and Adoptive T Cell Therapy. Cancer Cell 31: 711–23 e4 [PubMed: 28486109]
18. Ayers M, Lunceford J, Nebozhyn M, Murphy E, Loboda A, Kaufman DR, Albright A, Cheng JD, Kang SP, Shankaran V, Piha-Paul SA, Yearley J, Seiwert TY, Ribas A, McClanahan TK. 2017 IFN-gamma-related mRNA profile predicts clinical response to PD-1 blockade. J Clin Invest 127: 2930–40 [PubMed: 28650338]
19. Roulstone V, Pedersen M, Kyula J, Mansfield D, Khan AA, McEntee G, Wilkinson M, Karapanagiotou E, Coffey M, Marais R, Jebar A, Errington-Mais F, Melcher A, Vile R, Pandha H, McLaughlin M, Harrington KJ. 2015 BRAF- and MEK-Targeted Small Molecule Inhibitors Exert Enhanced Antimelanoma Effects in Combination With Oncolytic Reovirus Through ER Stress. Mol Ther 23: 931–42 [PubMed: 25619724]
20. Bagheri N, Shiina M, Lauffenburger DA, Korn WM. 2011 A dynamical systems model for combinatorial cancer therapy enhances oncolytic adenovirus efficacy by MEK-inhibition. PLoS Comput Biol 7: e1001085 [PubMed: 21379332]
21. Botta G, Passaro C, Libertini S, Abagnale A, Barbato S, Maione AS, Hallden G, Beguinot F, Formisano P, Portella G. 2012 Inhibition of autophagy enhances the effects of E1A-defective oncolytic adenovirus dl922–947 against glioma cells in vitro and in vivo. Hum Gene Ther 23: 623–34 [PubMed: 22475378]
22. Smith KD, Mezhir JJ, Bickenbach K, Veerapong J, Charron J, Posner MC, Roizman B, Weichselbaum RR. 2006 Activated MEK suppresses activation of PKR and enables efficient replication and in vivo oncolysis by Deltagamma(1)34.5 mutants of herpes simplex virus 1. J Virol 80: 1110–20 [PubMed: 16414988]
23. Veerapong J, Bickenbach KA, Shao MY, Smith KD, Posner MC, Roizman B, Weichselbaum RR. 2007 Systemic delivery of (gamma1)34.5-deleted herpes simplex virus-1 selectively targets and treats distant human xenograft tumors that express high MEK activity. Cancer Res 67: 8301–6 [PubMed: 17804745]
24. Gilmartin AG, Bleam MR, Groy A, Moss KG, Minthorn EA, Kulkarni SG, Rominger CM, Erskine S, Fisher KE, Yang J, Zappacosta F, Annan R, Sutton D, Laquerre SG. 2011 GSK1120212 (JTP-74057) is an inhibitor of MEK activity and activation with favorable pharmacokinetic properties for sustained in vivo pathway inhibition. Clin Cancer Res 17: 989–1000 [PubMed: 21245089]
25. Xia T, Konno H, Barber GN. 2016 Recurrent Loss of STING Signaling in Melanoma Correlates with Susceptibility to Viral Oncolysis. Cancer Res 76: 6747–59 [PubMed: 27680683]
26. Vella LJ, Pasam A, Dimopoulos N, Andrews M, Knights A, Puaux AL, Louahed J, Chen W, Woods K, Cebon JS. 2014 MEK inhibition, alone or in combination with BRAF inhibition, affects multiple functions of isolated normal human lymphocytes and dendritic cells. Cancer Immunol Res 2: 351–60 [PubMed: 24764582]
27. Itamura H, Shindo T, Tawara I, Kubota Y, Kariya R, Okada S, Komanduri KV, Kimura S. 2016 The MEK inhibitor trametinib separates murine graft-versus-host disease from graft-versus-tumor effects. JCI Insight 1: e86331 [PubMed: 27699218]
28. Woo SR, Fuertes MB, Corrales L, Spranger S, Furdyna MJ, Leung MY, Duggan R, Wang Y, Barber GN, Fitzgerald KA, Alegre ML, Gajewski TF. 2014 STING-dependent cytosolic DNA

sensing mediates innate immune recognition of immunogenic tumors. Immunity 41: 830–42 [PubMed: 25517615]

29. Kaufman HL, Kim DW, DeRaffele G, Mitcham J, Coffin RS, Kim-Schulze S. 2010 Local and distant immunity induced by intralesional vaccination with an oncolytic herpes virus encoding GM-CSF in patients with stage IIIc and IV melanoma. Ann Surg Oncol 17: 718–30 [PubMed: 19915919]
30. Terawaki S, Chikuma S, Shibayama S, Hayashi T, Yoshida T, Okazaki T, Honjo T. 2011 IFN-alpha directly promotes programmed cell death-1 transcription and limits the duration of T cell-mediated immunity. J Immunol 186: 2772–9 [PubMed: 21263073]
31. Chevolet I, Speeckaert R, Schreuer M, Neyns B, Krysko O, Bachert C, Hennart B, Allorge D, van Geel N, Van Gele M, Brochez L. 2015 Characterization of the in vivo immune network of IDO, tryptophan metabolism, PD-L1, and CTLA-4 in circulating immune cells in melanoma. Oncoimmunology 4: e982382 [PubMed: 25949897]
32. Deken MA, Gadiot J, Jordanova ES, Lacroix R, van Gool M, Kroon P, Pineda C, Geukes Foppen MH, Scolyer R, Song JY, Verbrugge I, Hoeller C, Dummer R, Haanen JB, Long GV, Blank CU. 2016 Targeting the MAPK and PI3K pathways in combination with PD1 blockade in melanoma. Oncoimmunology 5: e1238557 [PubMed: 28123875]
33. Corrales L, Matson V, Flood B, Spranger S, Gajewski TF. 2017 Innate immune signaling and regulation in cancer immunotherapy. Cell Res 27: 96–108 [PubMed: 27981969]
34. Toda M, Rabkin SD, Kojima H, Martuza RL. 1999 Herpes simplex virus as an in situ cancer vaccine for the induction of specific anti-tumor immunity. Hum Gene Ther 10: 385–93 [PubMed: 10048391]
35. Disis ML, Wallace DR, Gooley TA, Dang Y, Slota M, Lu H, Coveler AL, Childs JS, Higgins DM, Fintak PA, dela Rosa C, Tietje K, Link J, Waisman J, Salazar LG. 2009 Concurrent trastuzumab and HER2/neu-specific vaccination in patients with metastatic breast cancer. J Clin Oncol 27: 4685–92 [PubMed: 19720923]
36. Memarnejadian A, Meilleur CE, Shaler CR, Khazaie K, Bennink JR, Schell TD, Haeryfar SMM. 2017 PD-1 Blockade Promotes Epitope Spreading in Anticancer CD8(+) T Cell Responses by Preventing Fratricidal Death of Subdominant Clones To Relieve Immunodomination. J Immunol 199: 3348–59 [PubMed: 28939757]
37. Kawaguchi K, Igarashi K, Murakami T, Zhao M, Zhang Y, Chmielowski B, Kiyuna T, Nelson SD, Russell TA, Dry SM, Li Y, Unno M, Eilber FC, Hoffman RM. 2017 Tumor-Targeting Salmonella typhimurium A1-R Sensitizes Melanoma With a BRAF-V600E Mutation to Vemurafenib in a Patient-Derived Orthotopic Xenograft (PDOX) Nude Mouse Model. J Cell Biochem 118: 2314–9 [PubMed: 28106277]
38. Bommareddy PK, Patel A, Hossain S, Kaufman HL. 2017 Talimogene Laherparepvec (T-VEC) and Other Oncolytic Viruses for the Treatment of Melanoma. Am J Clin Dermatol 18: 1–15 [PubMed: 27988837]

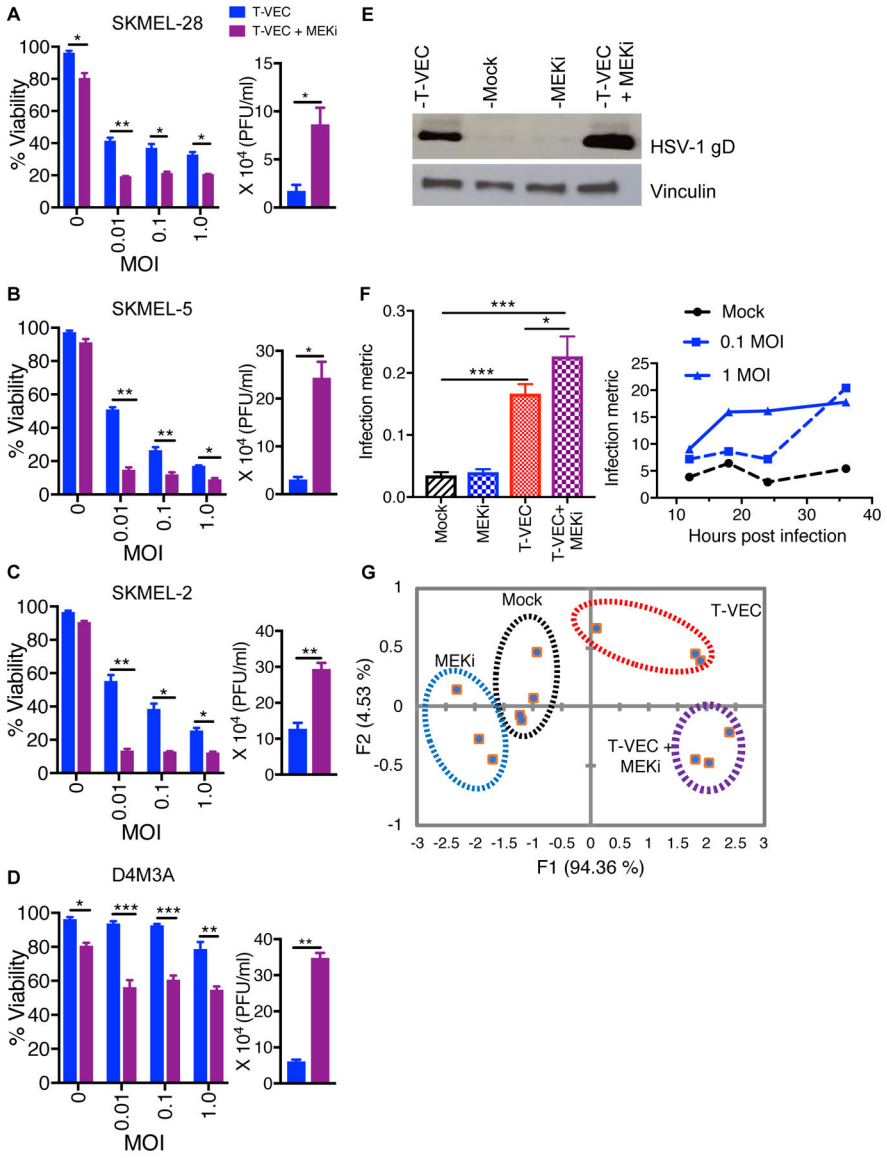

Figure 1. MEK inhibition augments T-VEC-mediated cell lysis *in vitro* and increases viral replication.

Cell viability determined by MTS assay. Cells were treated with either T-VEC alone or trametininb or combination T-VEC and trametinib **(A-D**, left panels**)**. The right panels (**A-D**) show HSV-1 titers as measured by plaque assay from cells treated with either T-VEC alone (blue bar) or T-VEC and trametinib (purple bar). Only significant differences are indicated. **(E)** Western blot of cell lysate collected at 24 hours after mT-VEC (0.1 MOI) infection of SK-MEL-28, mock infected, MEKi (10 nM) or combination treatment. **(F)** Infection metric analysis by Lumacyte (left panel) of SK-MEL-28 cells (mock), treated with 10 nM trametinib (MEKi), 1 MOI T-VEC or trametinib and T-VEC. The right panel shows a time course for untreated cells (black line), or those treated with 0.1 MOI of T-VEC (dotted blue line) or 1 MOI of T-VEC (solid blue line). **(G)** Principle component analysis (PCA) of the infection metric. Each experiment was performed in triplicates and is conducted at least twice with similar results. Data are presented as mean ± SEM and statistical differences

between groups was measured by using two-tailed student *t* test. *p < 0.05, **p < 0.01, ***p < 0.001, ****p < 0.0001.

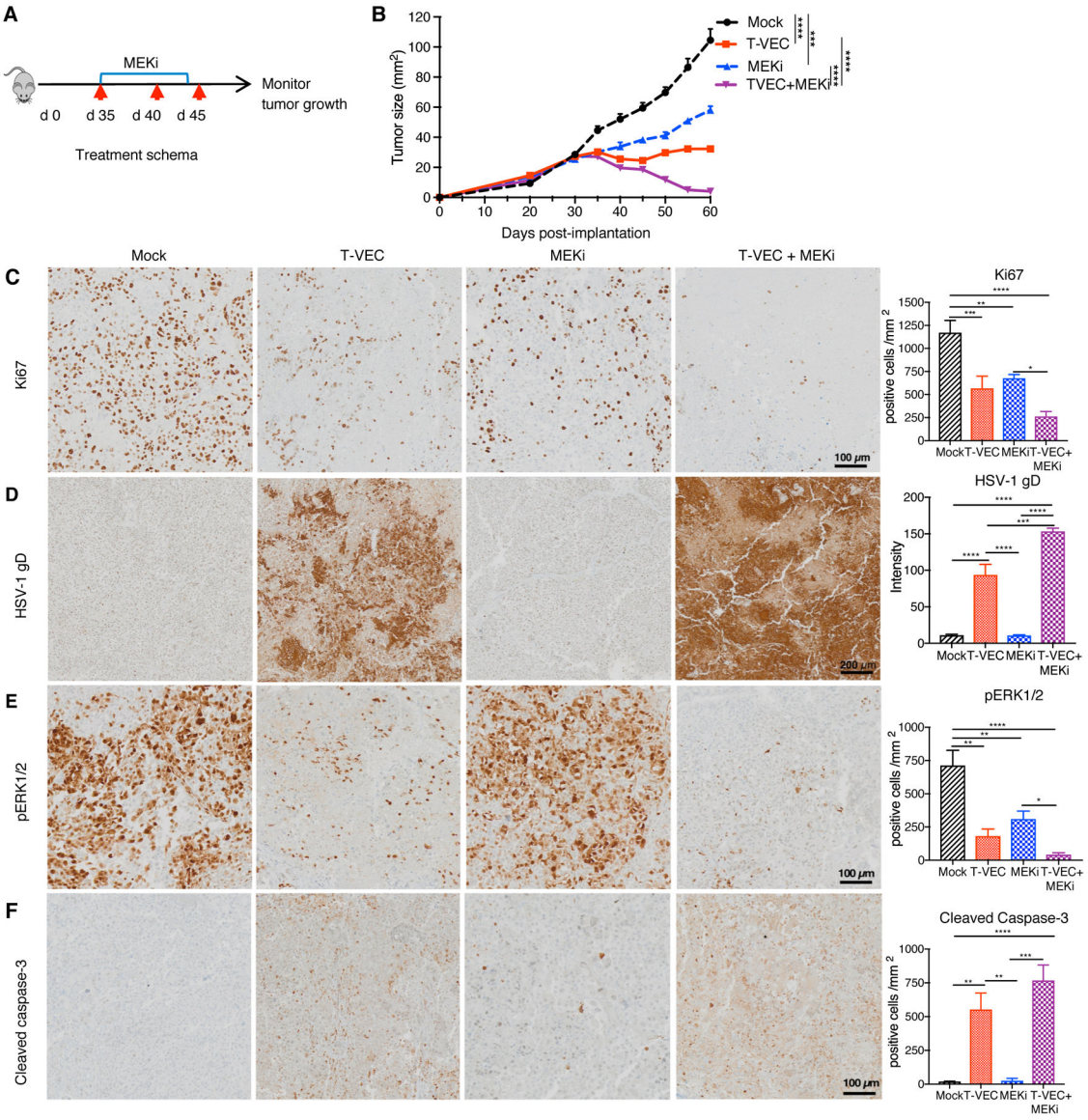

Figure 2. MEK inhibition enhances T-VEC-induced inhibition of human melanoma xenograft growth *in vivo* and promotes tumor cell apoptosis.

(A) NSG mice (n = 5/group) were implanted subcutaneously (s.c.) with human melanoma SK-MEL-28 cells (8×10^6) on day 0, treated via intratumoral (i.t.) injection with sterile water or T-VEC (1×10^5 pfu) on days 35, 40 and 45, and MEKi (trametinib; 0.5 mg/kg) or vehicle (0.2% Tween 80 and 0.5% hydroxypropyl methyl cellulose (HPMC) was given from days 35–43 via oral gavage. Red arrows indicate days when T-VEC was injected and top blue bar indicates days of trametinib (MEKi) treatment. **(B)** Mean tumor area. (**C**) Representative images obtained from immunohistochemical staining of tumors for Ki67 at day 36; **(D)** HSV-1 gD; **(E)** pERK1/2; and **(F)** cleaved caspase 3. Right panels indicate quantification of positive cells. Scale bars are as indicated Each experiment was repeated at least twice with similar results. Data are presented as mean ± SEM and statistical differences between groups was measured by using one-way ANOVA. *p < 0.05, **p < 0.01, ***p < 0.001, ****p < 0.0001. Only significant differences are indicated.

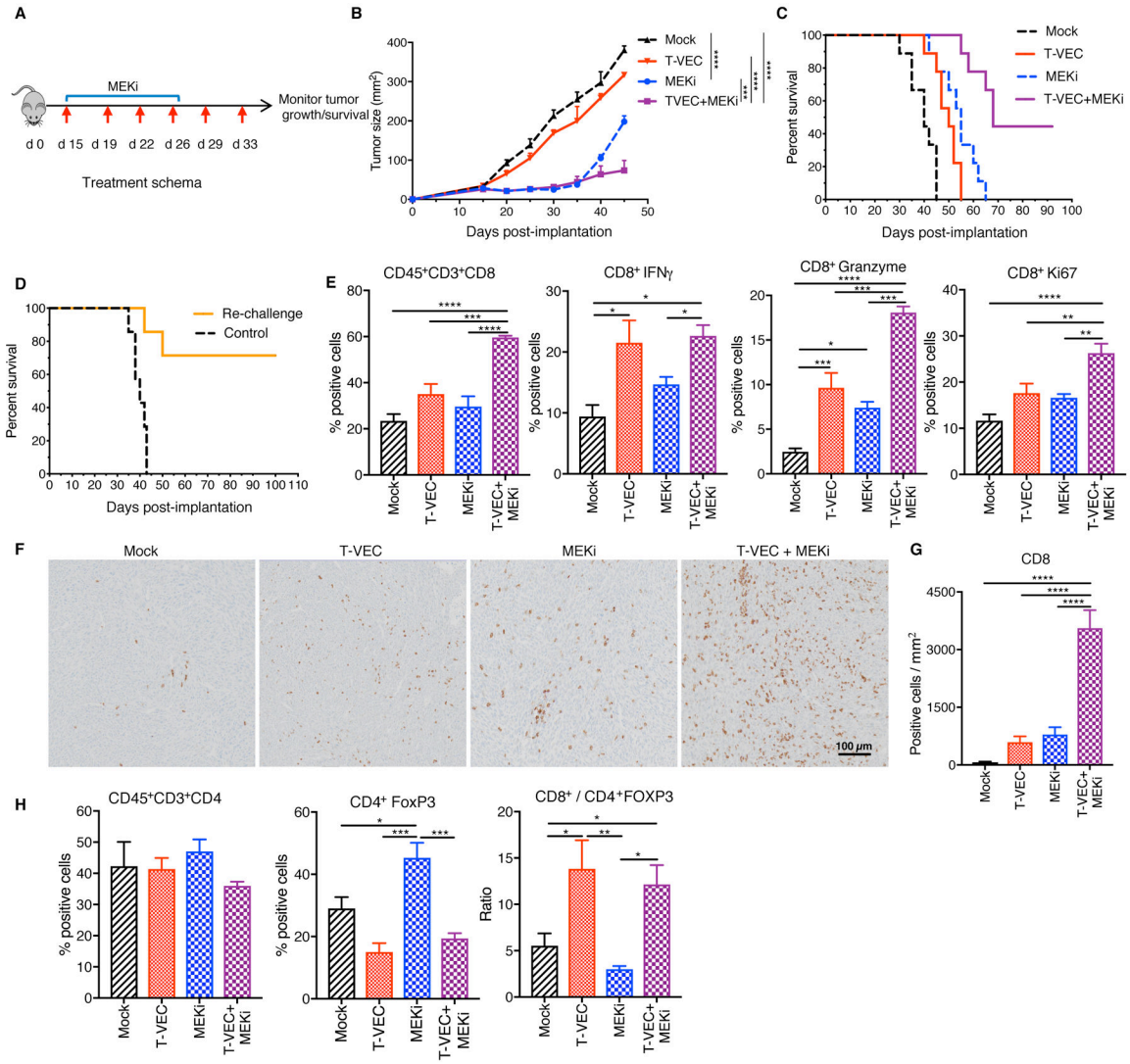

Figure 3. MEK inhibition enhances T-VEC-induced tumor regression in an immune competent murine melanoma model, promotes recruitment of CD8+ T cells and establishes long-term memory.

(A) Treatment schema: red arrows indicate days of mT-VEC treatment and top blue bar indicates trametinib (MEKi) treatment. **(B)** Mean tumor area of mice from treated groups at day 45. **(C)** Survival of mice. **(D)** Re-challenge of mice cured in 3C. **(E-F)** Flow cytometry analysis of tumors at day 24. **(E)** Bar graphs (n=6) indicating the percent positive CD8 T cells, CD8+IFN-γ, CD8+GranzymeB, and CD8+Ki67 T cells respectively. **(F)** Immunohistochemical staining of CD8+ T cells in the tumor. Scale bar as indicted. **(G)** Quantification of CD8 positive cells. **(H)** Bar graph indicating $CD4^+$ and $CD4^+$FoxP3 (Treg's) and ratio of CD8+ T cells to Tregs. Each experiment was conducted at least twice with similar results. Data are presented as mean ± SEM and statistical differences between groups was measured by using one-way ANOVA. *p < 0.05, **p < 0.01, ***p < 0.001, ****p < 0.0001. Only significant differences are indicated.

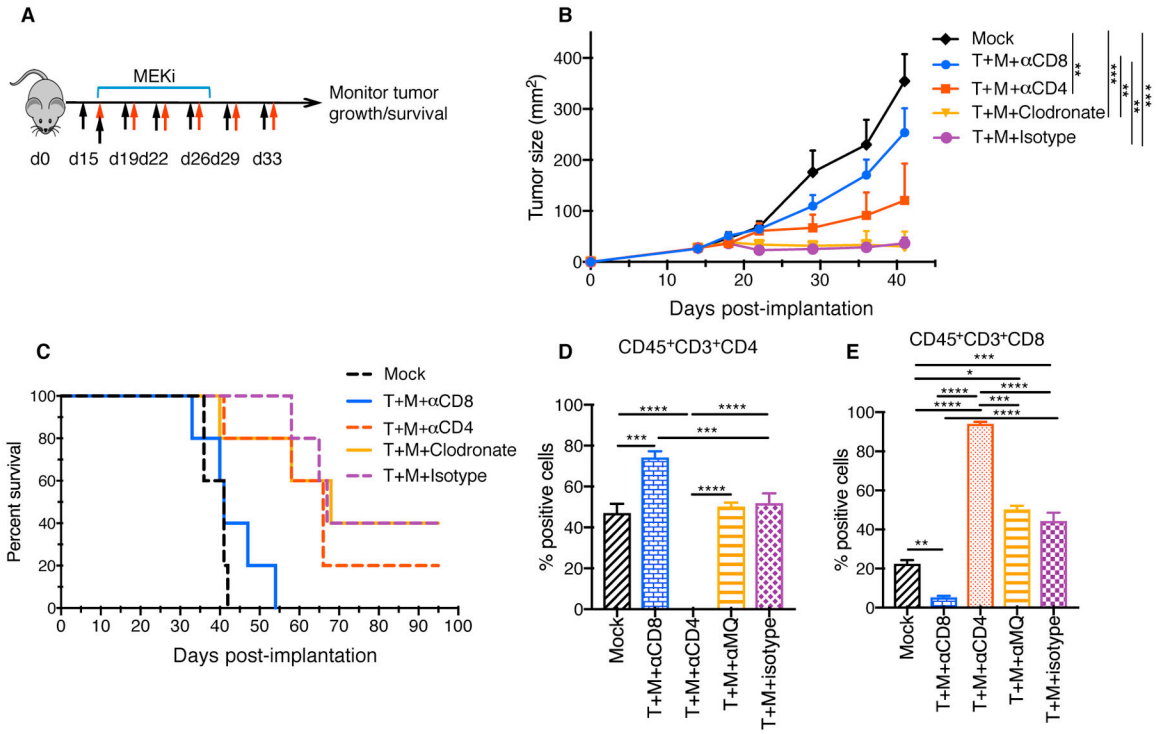

Figure 4. Depletion of CD8$^+$ T cells abrogates the effects of T-VEC and MEKi combination therapy.

(A) C57BL/6J mice (n = 5/group) were implanted with D4M3A murine melanoma cells and mice were treated as indicated, described in methods. Red arrows indicate days of mT-VEC treatment, top blue bar indicated days of trametinib (MEKi) treatment, and black arrows indicating days where depletion antibodies against CD4, CD8 and clodronate were injected. (**B**) Mean tumor area of mice treated from different groups as indicated at day 40. (**C**) Survival of mice. **(D-E)** Flow cytometric analysis of tumor infiltrating T cells on day 24. **(D)** Bar graphs show the percentage CD45$^+$CD3$^+$CD4+ and **(E)** CD45$^+$CD3$^+$CD8+ cells. Each experiment was repeated at least twice with similar results. Data are presented as mean ± SEM and statistical differences between groups was measured by using one-way ANOVA. *p < 0.05, **p < 0.01, ***p < 0.001, ****p < 0.0001. Only significant differences are indicated.

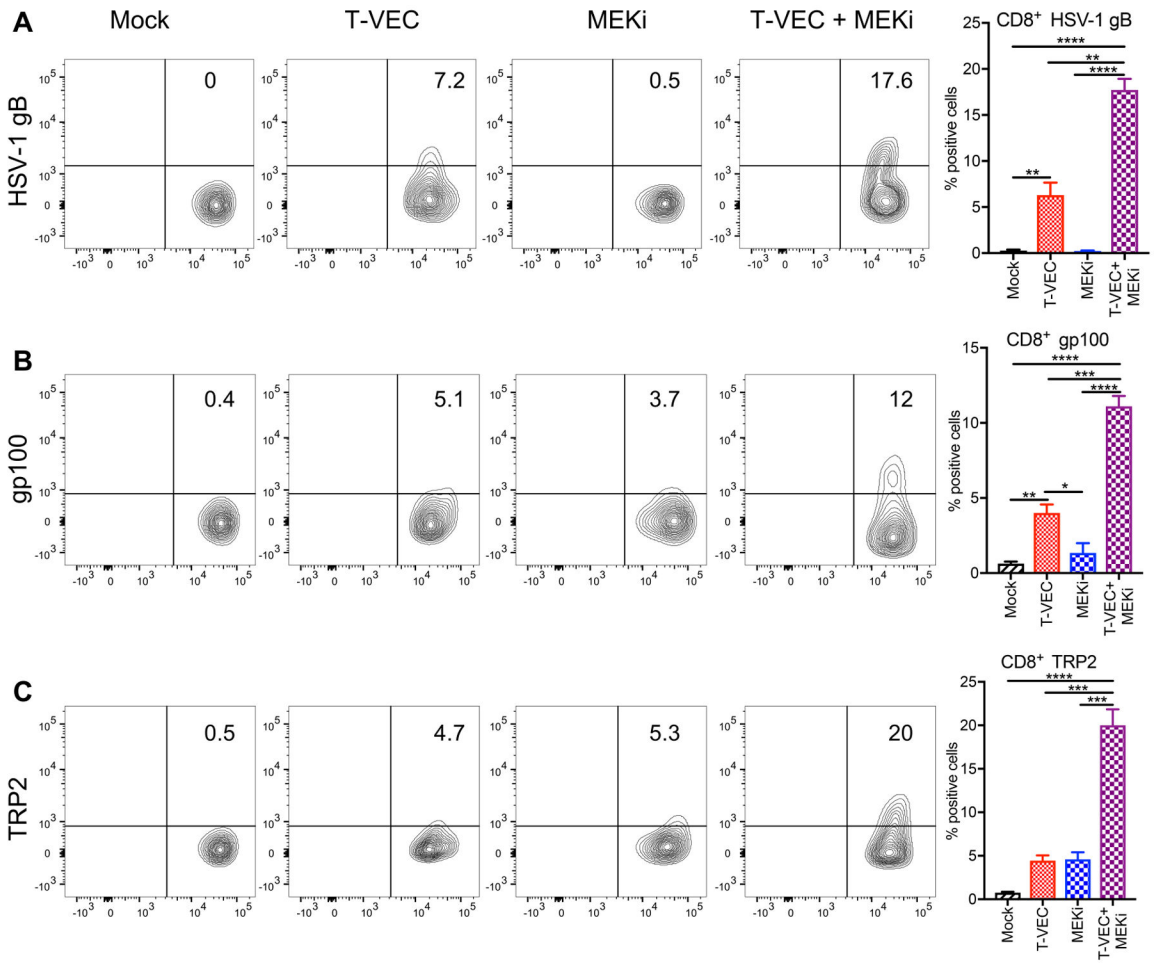

Figure 5. Combination T-VEC and MEK inhibition induces viral-specific CD8+ T cells and increases melanoma antigen-specific CD8+ T cell responses.

C57BL/6J mice implanted s.c. in the right flank with 3×10^5 D4M3A cells and treated with mT-VEC (1×10^6 pfu) or sterile water i.t. for 3 doses on days 15, 19 and 22 and or trametinib (0.5 mg/kg) or vehicle (0.2% Tween 80 and 0.5% Hydroxypropyl methyl cellulose) orally once daily on days 15–19. Tumors were harvested on day 24, cells dissociated and analyzed by flow cytometry. Percentages of live CD45+ cells, CD3+ cells, and CD3+ sorted CD4+ and CD8+ subsets from the Mock, T-VEC monotherapy, MEKi monotherapy, and T-VEC + MEKi combination groups were analyzed and compared. Tumor-infiltrating CD8+ T cells were analyzed with **(A)** HSV-1-specific H-2K^b-HSV-1gB dextramer, **(B)** melanoma antigen specific H-2D^b-gp100 dextramer, **(C)** H-2K^b-TRP2 dextramers. Quantitative analysis is shown in the bar graphs on the right. These experiments were conducted at least twice with similar results. Data are presented as mean ± SEM and statistical differences between groups was measured by using one-way ANOVA. *$p < 0.05$, **$p < 0.01$, ***$p < 0.001$, ****$p < 0.0001$. Only significant differences are indicated.

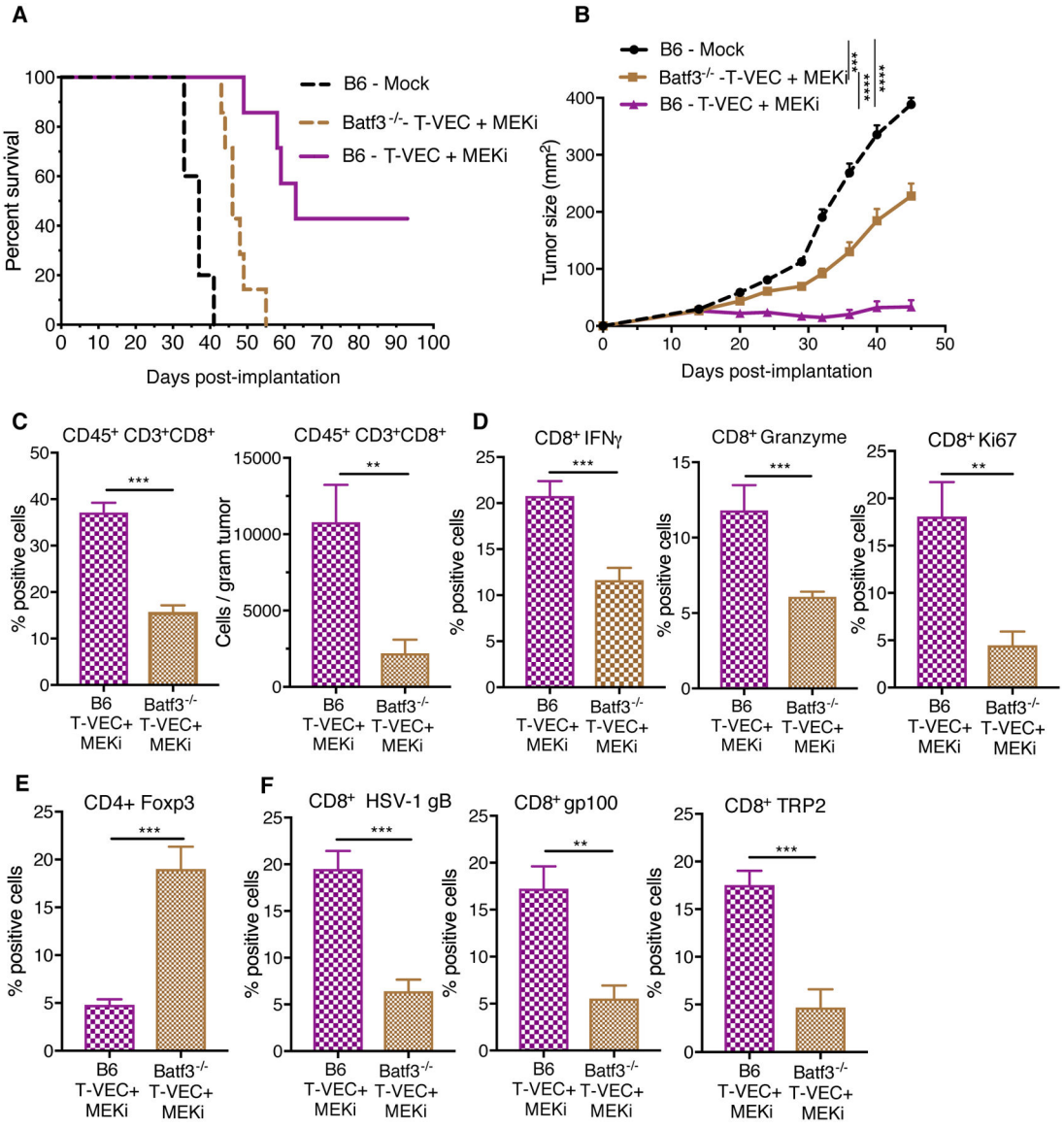

Figure 6. Batf3+ dendritic cells play a role in the anti-tumor activity and antigen spreading associated with combination T-VEC and MEK inhibition treatment.

C57BL/6J mice (B6, n = 7) and Batf3$^{-/-}$ mice (n = 7) were implanted with D4M3A murine melanoma cells and either mock treated or treated with T-VEC and trametininb as described in Materials and Methods. **(A)** Mean tumor area at day 45. **(B)** Survival of mice. **(C-F)** Flow cytometry analysis of tumors obtained from B6 and Batf3$^{-/-}$ mice on day 24. **(C)** Bar graph indicating the percentage, number, of tumor-infiltrating total CD8+ T cells and the frequency of CD8+IFN-γ+ and CD8+GranzymeB+ T cells respectively. **(D)** CD8+Ki67+ T cells. **(E)** CD4+FoxP3+ Tregs. **(F)** Percentage of HSV1-gB+, murine gp100+ and TRP2+ CD8+ T cells respectively. These experiments were repeated at least twice with similar results. Data presented as mean ± SEM and the statistical differences between groups was measured by two-tailed student *t* test. *p < 0.05, **p < 0.01, ***p < 0.001, ****p < 0.0001.

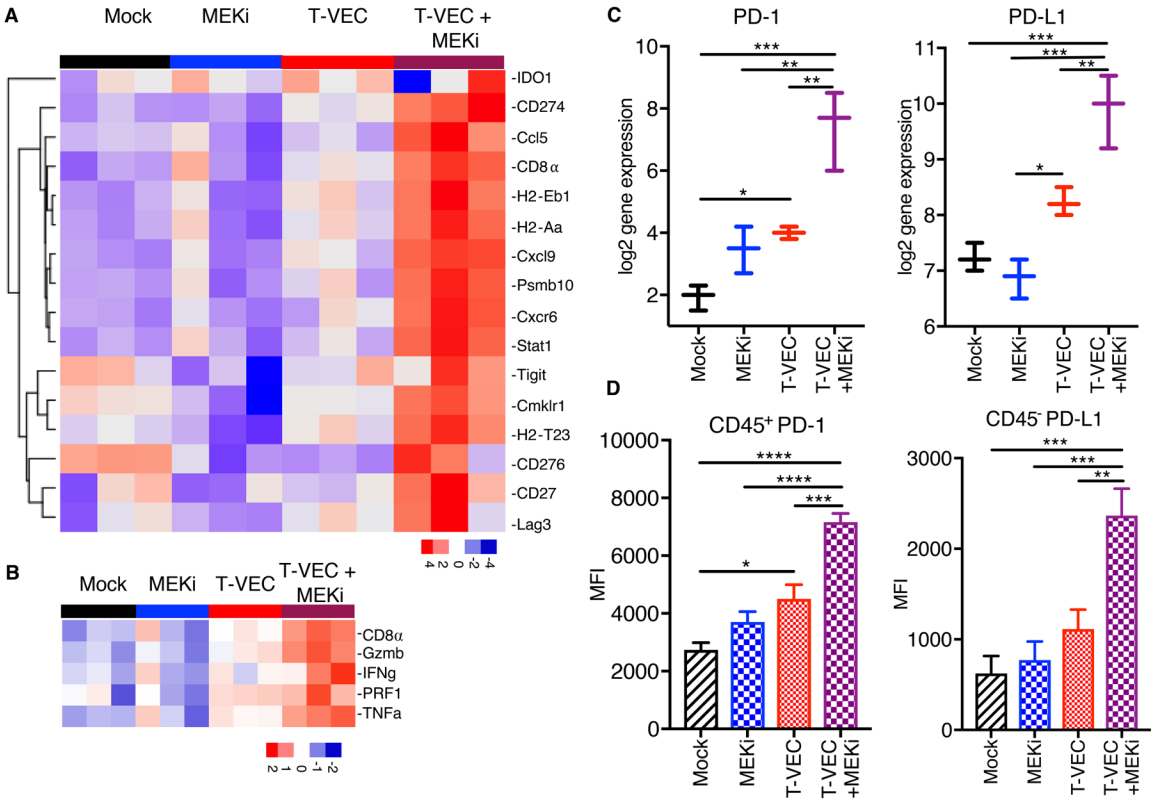

Figure 7. T-VEC and MEK inhibition reprograms immune silent tumors into immune inflamed tumors and induces expression of PD-1 and PD-L1.

C57BL/6J mice were implanted s.c. in the right flank with 3×10^5 D4M3A cells and treated with mT-VEC (1×10^6 pfu) i.t. for 3 doses on days 15, 19 and 22 and or trametinib (0.5 mg/kg) orally once daily on days 15–19. Tumors were harvested on day 24, total RNA was isolated and gene expression analysis performed using the NanoString PanCancer Immune panel as described in the Materials and Methods. **(A)** An inflammatory 16-gene expression profile was generated from mice (n=3) treated (as described in Fig 3D) with mock control (black), trametinib alone (MEKi; blue), mT-VEC alone (red), or combination mT-VEC and MEKi (purple). **(B)** A selected 5-gene expression signature represented by genes highly associated with $CD8^+$ T cell activation. **(C)** Gene expression of PD-1 (right panel) and PD-L1 (left panel). **(D)** Bar graphs show the mean fluorescence intensity (MFI) of CD45+PD-1+ (left panel) and CD45-PD-L1+ (right panel). Each experiment was performed at least twice with similar results. Data are presented as mean ± SEM and the statistical differences between groups were measured by two-tailed student *t* test. *p < 0.05, **p < 0.01, ***p < 0.001, ****p < 0.0001.

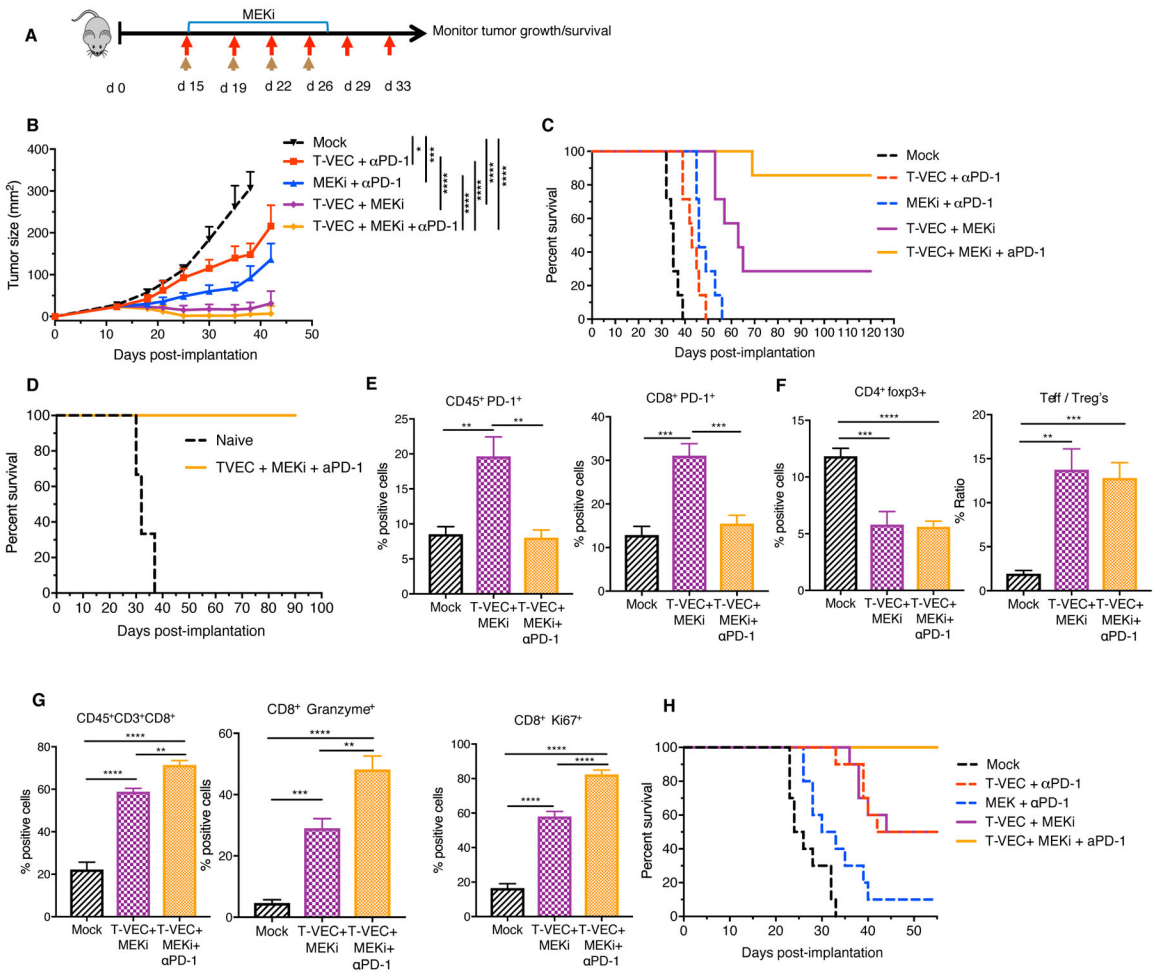

Figure 8. Triple combination treatment with T-VEC, MEK inhibition and PD-1 blockade improves therapeutic treatment of melanoma and colon cancer models.

(A) Treatment schema: red arrows indicate T-VEC, top blue bar indicates trametinib and brown arrows indicate αPD-1. **(B)** Mean tumor area. **(C)** Survival of mice. **(D)** Re-challenge of mice cured from B. **(E-F)** Flow cytometry of tumors at day 24. Bar graph indicating percent positive **(E)** CD45+PD-1+ cells (right panel) and CD45+CD8+PD-1+ cells (left panel), **(F)** CD4+FoxP3+ (right panel) and ratio of effector T cells to Tregs (left panel **(G)** CD8+ T cells, granzyme B+ CD8 T cells, and Ki67+ CD8 T cells respectively. **(H)** Evaluation of triple combination in CT26 murine colon carcinoma model. Mice were treated as described in Materials and Methods. Each experiment was conducted at least twice with similar results. Data are presented as mean ± SEM and statistical differences between groups were measured by two-tailed student *t* test. *p < 0.05, **p < 0.01, ***p < 0.001, ****p < 0.0001.